

Article

Determine the Land-Use Land-Cover Changes, Urban Expansion and Their Driving Factors for Sustainable Development in Gazipur Bangladesh

Hossain Mohammad Arifeen¹, Khamphe Phoungthong^{1,2}, Ali Mostafaeipour^{1,2,3}, Nuttaya Yuangyai⁴, Chumpol Yuangyai⁵, Kuaanan Techato^{1,2} and Warangkana Jutidamrongphan^{1,2,*}

¹ Faculty of Environmental Management, Prince of Songkla University, Hat Yai 90110, Thailand; 6210930003@email.psu.ac.th (H.M.A.); khamphe.p@psu.ac.th (K.P.); mostafaei@yazd.ac.ir (A.M.); kuaanan.t@psu.ac.th (K.T.)

² Environmental Assessment and Technology for Hazardous Waste Management Research Center, Faculty of Environmental Management, Prince of Songkla University, Songkhla 90110, Thailand

³ Industrial Engineering Department, Yazd University, Yazd 89195-741, Iran

⁴ Faculty of Liberal Arts and Management Sciences, Surat Thani Campus, Prince of Songkla University, 31 Moo 6, Makham Tia Subdistrict, Mueang District 84000, Thailand; nuttaya.y@psu.ac.th

⁵ Department of Industrial Engineering, School of Engineering, King Mongkut's Institute of Technology Ladkrabang, Bangkok 10520, Thailand; chumpol.yu@kmitl.ac.th

* Correspondence: warangkana.j@psu.ac.th



Citation: Arifeen, H.M.; Phoungthong, K.; Mostafaeipour, A.; Yuangyai, N.; Yuangyai, C.; Techato, K.; Jutidamrongphan, W. Determine the Land-Use Land-Cover Changes, Urban Expansion and Their Driving Factors for Sustainable Development in Gazipur Bangladesh. *Atmosphere* **2021**, *12*, 1353. <https://doi.org/10.3390/atmos12101353>

Academic Editors: Yaoping Cui and Abhnil Prasad

Received: 17 September 2021

Accepted: 12 October 2021

Published: 16 October 2021

Publisher's Note: MDPI stays neutral with regard to jurisdictional claims in published maps and institutional affiliations.



Copyright: © 2021 by the authors. Licensee MDPI, Basel, Switzerland. This article is an open access article distributed under the terms and conditions of the Creative Commons Attribution (CC BY) license (<https://creativecommons.org/licenses/by/4.0/>).

Abstract: At present, urbanization is a very common phenomenon around the world, especially in developing countries, and has a significant impact on the land-use/land-cover of specific areas, producing some unwanted effects. Bangladesh is a tightly inhabited country whose urban population is increasing every day due to the expansion of infrastructure and industry. This study explores the land-use/land-cover change detection and urban dynamics of Gazipur district, Bangladesh, a newly developed industrial hub and city corporation, by using satellite imagery covering every 10-year interval over the period from 1990 to 2020. Supervised classification with a maximum likelihood classifier was used to gather spatial and temporal information from Landsat 5 (TM), 7 (ETM+) and 8 (OLI/TIRS) images. The Geographical Information System (GIS) methodology was also employed to detect changes over time. The kappa coefficient ranged between 0.75 and 0.90. The agricultural land was observed to be shrinking very rapidly, with an area of 716 km² in 2020. Urbanization increased rapidly in this area, and the urban area grew by more than 500% during the study period. The urbanized area expanded along major roads such as the Dhaka–Mymensingh Highway and Dhaka bypass road. The urbanized area was, moreover, concentrated near the boundary line of Dhaka, the capital city of Bangladesh. Urban expansion was found to be influenced by demographic-, economic-, location- and accessibility-related factors. Therefore, similarly to many countries, concrete urban and development policies should be formulated to preserve the environment and, thereby, achieve sustainable development goal (SDG) 11 (sustainable cities and communities).

Keywords: land-use/land-cover; urban growth; Geographical Information System; sustainable development; supervised classification

1. Introduction

Global economic growth has been observed in recent years, leading to worry about the effects of globalization on neighboring regions [1–3]. Urbanization that takes place on the urban periphery, due to its unpredictable consequences, can affect the sustainability of the area. Several variables are responsible for the rise and development of a major city and its relationship with the Peri-Urban Area (PUA), including economic development, the intensity of trade expansion and the political motivation of the state [4].

The share of urban population in the world rose from 14% in 1900 to 29.1% in 1950 and 54% in 2014; the global urban population is projected to total 66% by 2050 [5]. The expansion of urban centers in emerging nations has prompted a shift from compact and interconnected cities to sprawling, uncontrolled urban development. This phenomenon means that metropolitan areas are fraught with many new difficulties that planners, governors and legislators must contend with. The effects of these changes in terms of land use and land cover, as well as urban sprawl, represent a major issue [6–8]. Confirmed data on land-pattern changes are necessary to achieve ongoing growth and correctly manage natural properties. These are also essential factors for many environmental functions. Fundamentally, the words comprising Land use land cover are not same, but they are often used in similar and alternative senses. “Land cover” is used to indicate the natural settings of the Earth’s exterior, including the spread of forestry, crop fields, etc. In contrast, land use denotes anthropogenic interventions primarily motivated by economic issues [9].

Launched in July 1972, the Earth Resource Technology Satellite (ERTS) 1 (later known as Landsat 1) has made a significant contribution to the development of remote sensing applications, including land cover classification [10,11]. These developments emerged as a result of improvements to Landsat images and computer technology, the development of geographic information systems (GIS) and the policy of Landsat’s open access. Landsat images have been used to categorize land cover over the last four decades. Land cover refers to the physical materials that cover the Earth’s surface, such as forests, lakes and grasslands. Thus, in order to classify land cover, one must use different classification methods developed in the field of remote sensing. As a result of the Landsat data access policy change in 2008, as well as the development of high-performance computer capabilities, these remote sensing classification methods have been applied to an increasingly wider variety of Landsat images. Recently, Landsat-based land-cover classification methods have become a hot topic, especially given the current effects of climate change [12]. Fast remote-sensing-based LULC mapping is now available and offers high accuracy at a reduced price [13]. Remote sensing is a dynamic tool that provides valuable information series covering both time and space in detail [14]. A global positioning system (GPS) is an important device used to gather field data as reference data to calibrate a classification or in a Geographic Information System for mapping [15]. The latest developments in geographic information science, remote sensing technology and digitalization, particularly with the advent of ground-breaking machine learning and deep learning algorithms, have created new ways to improve current processes and resolve land-use and land-cover issues. Furthermore, the maximum likelihood classifier (MLC) has been widely used and is now a well-accepted methodology. Several previous studies were conducted in this area [16–18].

Diverse factors are responsible for the changing patterns of land use and land cover around the world. Anthropogenic and socio-economic issues have been commonly highlighted as decisive elements in diversification. The petroleum industry and various types of structures are major players that affected the land-use patterns in Sekondi–Takoradi, Ghana [6], over the last three decades (1986–2016). A study in [6] also indicated that a shrinkage of crop land would be the ultimate result, possibly leading to poverty. This result would conflict with Sustainable Development Goal (SDG) one (End poverty in all its forms everywhere) as declared by the United Nations. The dominant factors in Shanghai, China [19], were anthropogenic interventions and socio-economical behaviors. A study in Latvia [20] found that the areas near roads experienced massive LULC changes, while areas farther from the capital experienced fewer changes. Around the Mekong delta in Vietnam [21], the primary parameters causing changes to land classes included economic, socio-economic and demographic policies.

Several studies related to remote sensing and GIS have assessed different LULC aspects, focusing, e.g., on forest/vegetation [22,23] and agricultural land [24–26].

Despite the various perspectives on changing land patterns, in the last few years in developing countries, urbanization has been the primary factor responsible for changes in land use/land cover [27–29]. Almost one-half of the world’s population dwells in urban

areas. However, the total urban land area, at present, represents only three percent of the world's land surface [30,31]. With increases in urbanization, especially in developing countries, large research studies based on urban areas [32–35] have been executed to reflect actual urban scenarios.

GIS and remote-sensing applications in LULC assessments are relatively new in Bangladesh. Few studies have emphasized different land classes such as urban land and agricultural land. Dhaka, the capital of the country, has the highest priority for LULC assessment, as Dhaka is one of the largest and most densely populated cities in the world. LULC change detection of the Dhaka metropolitan city covering approximately half a century (1960–2005) revealed that urbanization squeezed out other land classes [36]. There was also another approach used to quantify the urban expansion of greater Dhaka [27]. This approach revealed the parameters responsible for facilitating urbanization, including altitude, demography and economical activities. Aside from these factors, few analyses have been conducted on ecological aspects. Such studies examined a Ramsar site [37] and a river catchment area [38].

Bangladesh is quickly moving toward further developments and achieved the status of a lower-middle-income country in 2015, with a GDP growth rate of 8.2% in 2019 [39]. Recently, the Bangladesh government proclaimed that the rural area would transform into an urban area. As Gazipur is the neighboring district to Dhaka, and this area is experiencing fast-paced development, Gazipur was selected for the current study. The primary objectives of this study were as follows:

- (1) Quantify and assess the overall land-use/land-cover changes in the Gazipur district, a rapidly developing industrial hub area in Bangladesh, over the period from 1990 to 2020;
- (2) Compute the changes in built-up areas in terms of both direction and distance during the time frame of 1990–2020;
- (3) Determine the major driving factors of land-use/land-cover changes, especially the reasons for the rapid progression of urbanization.

In brief, this research analyzes the land-use changes from the 1990s, when industrialization commenced in Bangladesh, to present. During this time frame, this area experienced urban development and became the largest city corporation in Bangladesh, where significant industrial activities have changed traditional land patterns. Moreover, the expansion of urban area in Bangladesh underscores the need for policy makers to develop foolproof policies to attain SDG 11 (Make cities and human settlements inclusive, resilient and sustainable).

The remainder of this article is formulated as follows. In the second section, the study area is described. In the third section, the materials and methods are presented. In the fourth section, the results are explained, and a discussion is developed. The fifth section is dedicated to urban expansion. In Section 6, the driving factors are presented. Finally, the conclusions are provided in Section 7.

2. Study Area

The study area is in Gazipur, which is located on the outskirts of Dhaka, Bangladesh. The district extends from 23°50' N to 24°20' N in latitude and from 90°10' E to 90°40' E in longitude (Figure 1). Gazipur is surrounded by the Mymensingh and Kishoreganj districts in the north, the Narshingdi district in the east, the Tangail district in the west and the Dhaka and Narayanganj districts in the south. Sitalakhya, Turag and Balu are the major rivers of the district. The Dhaka–Mymensingh Highway bisects the district in the north–south direction. The district contained around 1820 square kilometers of territory with approximately 3.5 million inhabitants in 2011 [40]. The population density in this area is high, at almost 1884 people/km². The population growth rate is 5.2% annually. The annual average temperature of this district ranges from a maximum of 36 °C to a minimum of 12.7 °C, and the annual rainfall is 2376 mm. The district consists of five upazila (subdistricts). The largest city corporation in Bangladesh is the 'Gazipur City

Corporation'. Moreover, this district contains three municipalities. "Vawal Pargana", the deepest forest of central Bangladesh, has been located in this area since ancient times. This area also has many industries, including thousands of garment factories, several education centers, many recreational places and government and private offices. This survey can serve as a model for future development in the north–south area of Bangladesh.

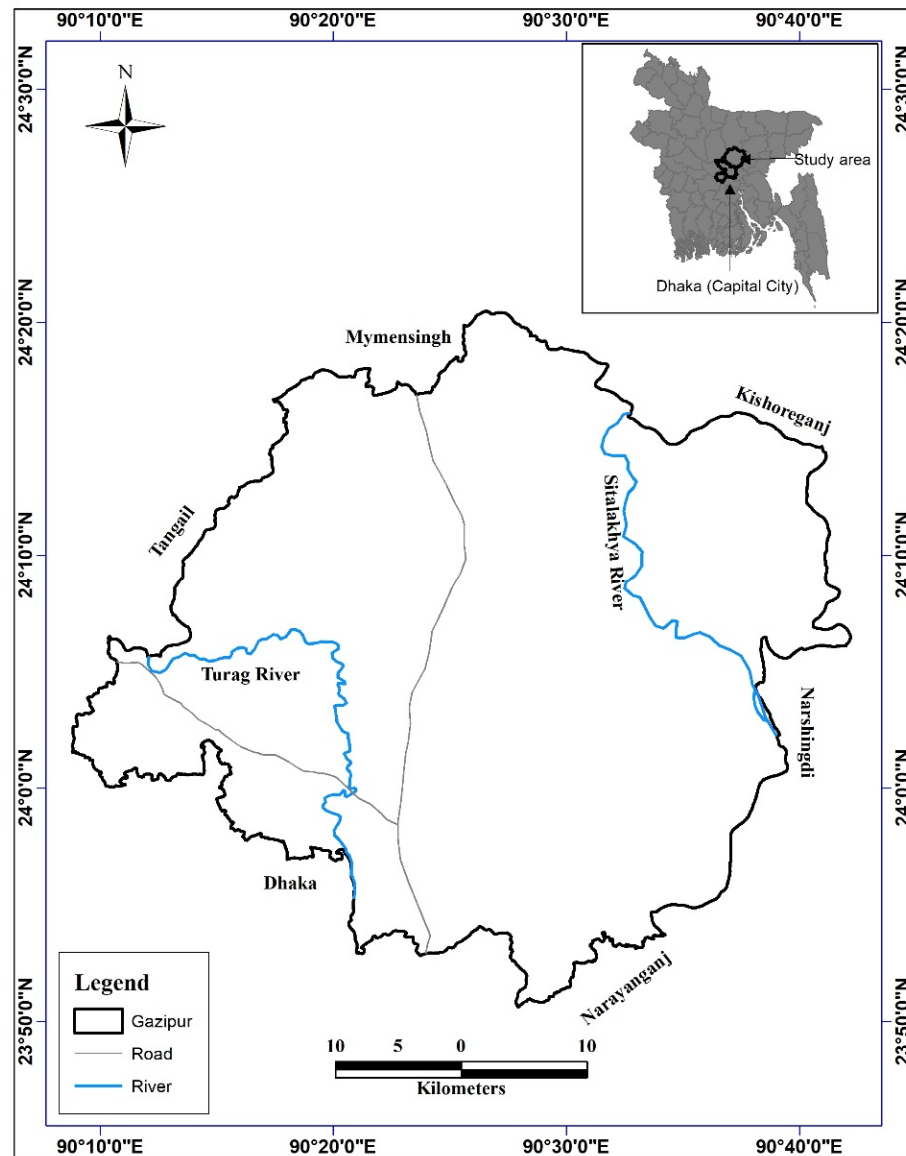


Figure 1. Location map of the study area.

3. Materials and Methods

3.1. Data

The present study engaged in a temporal analysis of satellite images from a fast-developing district adjacent to the capital city of Bangladesh. Thus, the first and foremost task was to select satellite sensors and associated images [41]. Landsat satellite images (Table 1) were ultimately selected for the experiment prior to the literature review of previous works.

Table 1. Image description.

Satellite Imagery	Acquisition Date	MS Bands	Description	Spatial Resolution
Landsat 5 TM	29 April 1990	Band 1–5, 7	Coastal and aerosol, vegetation and deciduous, peak vegetation, discriminates vegetation slopes, biomass content and shorelines, moisture content of soil and vegetation; penetrates thin clouds	30 m
Landsat 7 ETM+	2 February 2000	Band 1–5, 7	Coastal and aerosol, vegetation and deciduous, peak vegetation, discriminates vegetation slopes, biomass content and shorelines, moisture content of soil and vegetation; penetrates thin clouds	30 m
Landsat 5 TM	30 January 2010	Band 1–5, 7	Coastal and aerosol, vegetation and deciduous, peak vegetation, discriminates vegetation slopes, biomass content and shorelines, moisture content of soil and vegetation; penetrates thin clouds	30 m
Landsat8 OLI/TIRS	11 February 2020	Band 1–7	Coastal and aerosol, vegetation and deciduous, peak vegetation, discriminates vegetation slopes, biomass content and shorelines, moisture content of soil and vegetation; thermal mapping and estimated soil moisture; penetrates thin clouds	30 m

All the images were acquired from the United States Geological Survey’s image website, Earth Explorer (www.earthexplorer.usgs.gov accessed on 6 June 2020). The downloaded data covered a period from late January to the end of April (the dry season in Bangladesh) to keep the analysis free from the impacts of seasonal variability. The flight line that covered the area was path 43 and row 137.

The Landsat data are multi-spectral and used differently colored band layers. The Landsat Thematic Mapper (TM) images are composed of seven spectral bands, each with a spatial resolution of 30 m (bands 1–5 and 7). The spatial resolution of band 6 (thermal infrared) is 120 m. Enhanced Thematic Mapper Plus (ETM+) images are composed of eight spectral bands, each with a spatial resolution of 30 m (bands 1–7). All bands can collect one of two gain settings (high or low) to achieve enhanced radiometric sensitivity and a higher contrast ratio, except for band 6, which collects both high and low gain for all scenarios. An Operational Land Imager (OLI) and a Thermal Infrared Sensor (TIRS) were also employed in this study. The OLI and TIRS images consisted of nine spectral bands, with a spatial resolution of 30 m for bands 1 to 7, and included cover for various SWIR (short wave infrared—A wave length) segments. Such segments are very helpful in distinguishing between wet and dry soil, as well as different types of geology since rocks and soils that seem identical in other bands often exhibit sharp differences in SWIR.

3.2. Image Preprocessing

The image pre-processing and analysis involved several steps before generating the final output. The Earth Resource Development Association System (ERDAS) Imagine 2014 software was used to accomplish the preprocessing tasks. After downloading the images from Earth Explorer, the layer-stacking tool of the ERDAS Imagine software was utilized to merge the bands in the RGB format for all images (from 1990, 2000, 2010 and 2020). Then, with the help of the study area’s shape file, the images were divided into subsets for classification and further processing tasks.

3.3. Image Classification

Image classification is the most important task for land-use/land-cover change detection and quantification when employing remote sensing techniques. This task is defined as the bunching of pixels to similar data types that are generated from a few spectral bands of satellite imagery [41–43].

Supervised image classification with the Maximum Likelihood Classifier (MLC) was performed to obtain the land classes, as this is the most common and extensively used remote sensing-based classification algorithm [44]. Three types of Landsat images (5, 7 and 8), with a combination of bands 4–3–2 (NIR-R-G) for Landsat 5 (TM) and 7 (ETM+) images and 5–4–3 (NIR-R-G) for Landsat 8 (OLI) images, were used for processing due to their effectiveness in land-use mapping [45]. Approximately 300 points were selected for land-use classification using field work-based GPS (Ground Positioning System) data, as well as data collected from image interpretation for 2020. In total, 70% of the field data were used for training, and the rest were utilized for the accuracy assessment [46]. For 1990, 2000 and 2010, training samples were created from the images by using field data and expert knowledge. Utilizing the supervised algorithm method, signature files consisting of mean vectors and covariance matrices for each class were created first before running the classification results. These signatures were used with a classifier (maximum likelihood) to assign each pixel within the image to a discrete class.

It is common for misclassifications to occur in land cover classified using the supervised MLC algorithm, as more than one class label can produce similar types of reflectance, thereby confusing the classification calls. For instance, barren land is regularly confused with a built-up area. Improvements were achieved through post-classification refinements to minimize this problem and enhance accuracy, as such refinements were simple to perform [47]. It is notable that ground-truth experience was also necessary to complete the procedure.

A 3×3 majority filter was applied before further analysis of the classified land-use/land-covers to reduce the salt and pepper effect [48,49].

3.4. Land-Use Land-Cover Classification Scheme

Open access Landsat images are widely used around the world to assess and quantify land-use/land-cover variations from the micro to mega level and to record human-caused interruptions [50,51]. Precise land-class and land-use change data for analytical purposes are difficult to obtain, especially in built-up areas due to their diversified land characteristics and mixed pixels [52,53]. Barren land and impermeable developed areas commonly present similar types of spectral reflectivity, which is confusing and makes it difficult to correctly differentiate between these two land-use types [53,54]. The primary focus of the present research was to evaluate and detect the land-use/land-cover changes and spatial magnitude using time-series information. For this purpose, a first-order Anderson classification scheme [55] was employed, and six types of land classes were proposed (Table 2, Figure 2). The land classes were prepared based on expert analysis and ground investigations performed during September 2020.

Table 2. LULC classification scheme.

LULC Type	Description
Agriculture	Paddies, crops, vegetables, etc.
Vegetation	Natural vegetation, homesteads with trees (hfs), plantations, etc.
Built-up	Houses, shops, industries, paved surfaces, roads, etc.
Fallow land	Barren land, playgrounds, open fields, uncultivated land, sand-filling sites, brick fields, grazing fields, yard, waste-dumping sites, etc.
Low land	Marshy lands, seasonal channels, wetland, etc.
Water	Rivers, canals, ponds, etc.

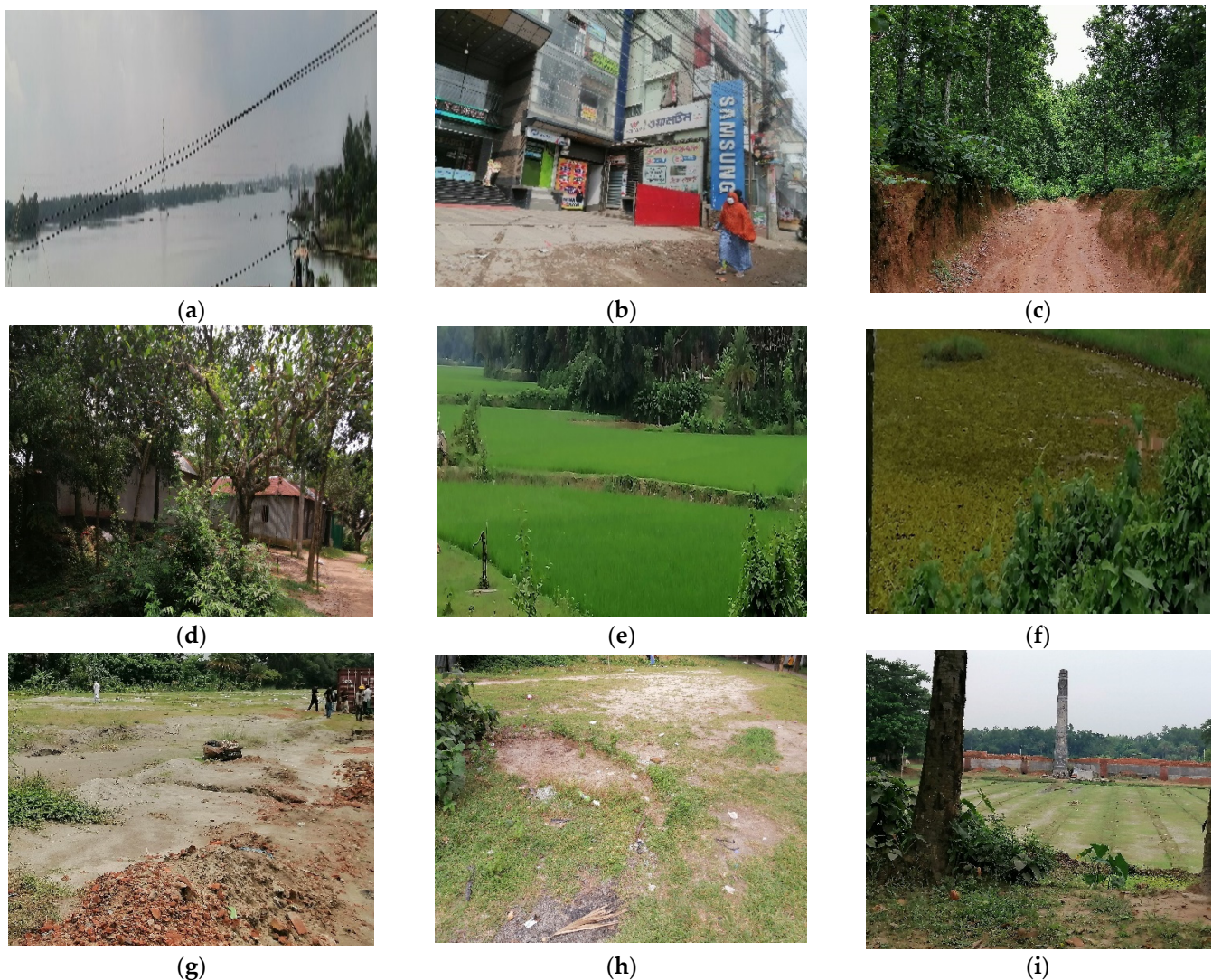


Figure 2. Different land classes (a–i). (a) Water; (b) Built-up; (c) Vegetation (Forest); (d) Vegetation (HFS); (e) Agriculture; (f) Low land; (g) Fallow land (Sand filled); (h) Fallow land (Barren); (i) Fallow land (Brick field).

3.5. Accuracy Assessment

Accuracy assessment is a very important step in image processing, especially in land-use/land-cover change detection. Such assessments have historically been performed using ground-truth data or by comparison using some selective points of previously classified maps [41]. To accomplish this task for 2020, 100 sampling points from the field and Google Earth were generated. To perform an accuracy assessment of the land-use/land-cover map for 2010, 2000 and 1990 and validate the accuracy, Google Earth was commissioned as a confirmation tool [56]. At present, Google Earth is a very useful and prevalent tool, and many researchers prescribe this tool as a means of validation.

In the accuracy assessment, the following formulae were applied:

$$\text{Overall accuracy} = \text{Total number of correctly classified pixels} / \text{Total reference pixels} \times 100 \quad (1)$$

$$\text{User accuracy} = \text{Number of correctly classified pixels} / \text{Total number of classified pixels (Row total)} \times 100 \quad (2)$$

$$\text{Producer accuracy} = \text{Number of correctly classified pixels} / \text{Total number of classified pixels (Column total)} \times 100 \quad (3)$$

$$\text{Kappa coefficient} = (\text{TS} \times \text{TCS}) - \sum (\text{Column total} \times \text{Row total}) / \text{TS}^2 - \sum (\text{Column total} \times \text{Row total}) \quad (4)$$

where TS is the total sample, and TCS is the total corrected sample.

3.6. Change Detection

The post-classification change analysis process was used to determine the changes in different land classes by applying the relevant formulae and performing a cross-tabulation investigation. The cross tabulation results illustrated the distribution and conversion of various land classes. The following formulae were applied to detect the changes in land-use/land-cover type over the given time span [57].

$$D_c = (A_{t_2} - A_{t_1}) / A_{t_1} \times 1 / (t_2 - t_1) \times 100\% \quad (5)$$

where D_c is the land-use dynamic degree, A_{t_1} represents the area of the land-use type at t_1 and A_{t_2} represents the area of this land-use type at t_2 .

$$C = (A_{t_2} - A_{t_1}) / A_{t_1} \times 100\% \quad (6)$$

where C is the area variation rate of land use, A_{t_1} represents the area of a land-use type at t_1 and A_{t_2} represents the area of this land-use type at t_2 .

Figure 3 summarizes the process in a flow chart.

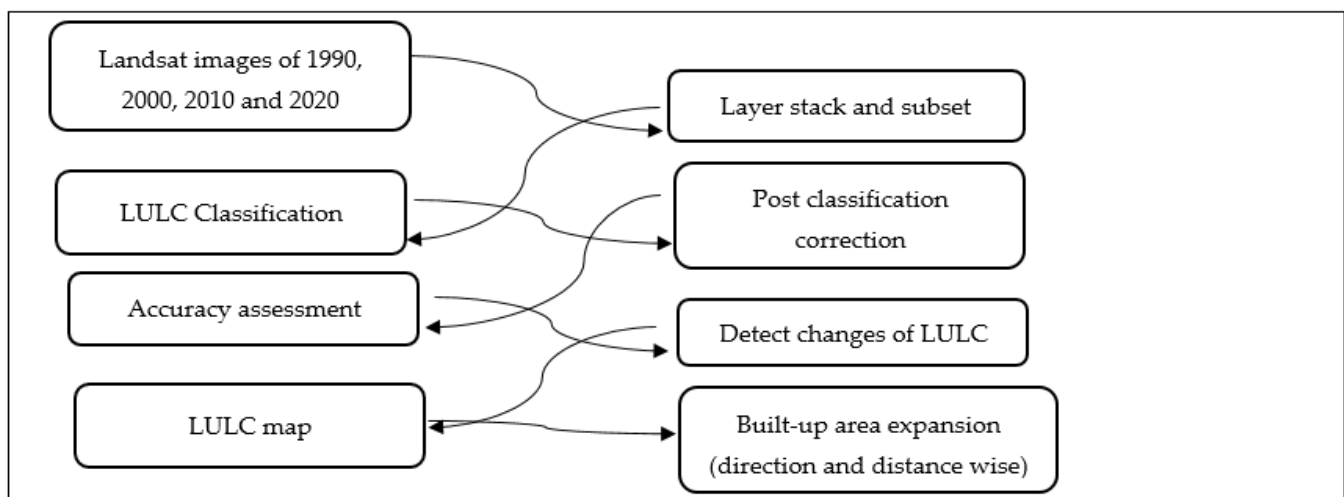


Figure 3. Flow chart of the work.

4. Results and Discussion

4.1. Accuracy

Validation, including overall accuracy and the Kappa coefficients, was performed on the six classified land classes for the years 1990, 2000, 2010 and 2020 (Table 3). In the study, the overall accuracy was very good, ranging from 86 to 94%. The Kappa coefficient was also admissible, for which a range from 0.6 to 0.79 is considered moderate, 0.80 to 0.90 is considered strong and above 0.90 is considered almost perfect [58].

Table 3. Overall accuracy and kappa coefficients by year.

Year	Overall Accuracy	Kappa Coefficient
1990	86 %	0.75
2000	93%	0.80
2010	94%	0.88
2020	93%	0.90

4.2. Land-Use/Land-Cover Change

The classified maps of 1990, 2000, 2010 and 2020 (Figure 4, Table 4) reveal that the area was primarily dominated by agriculture and vegetation. Over time, however, the built-up area increased. In 1990, the major land classes were agriculture (981 km²) and

vegetation (591 km², 32%), while the built-up area was only 18 square kilometers. During this time period, the water-body size was 172 km², and low land and fallow land were negligible (21 and 38 km²). The agriculture and vegetation areas occupied 1382 and 354 km², respectively, in 2000, while the built-up area occupied 23 km². The water-body area totaled 43 km². Moreover, approximately 1211 km² of the area was covered by agricultural and vegetation land (430 km²) and water (65 km²), while the built-up area totaled about 90 km². Vegetation and agricultural land were similar in quantity in 2020 (696 and 717 km², respectively), followed by fallow land (224 km²), with a decrease in the area occupied by water (51.13 km²). The built-up area occupied 105 km². Notably, the increase in fallow land is temporary, as the area remains in a developing phase, and land filling and construction processes are ongoing in the area.

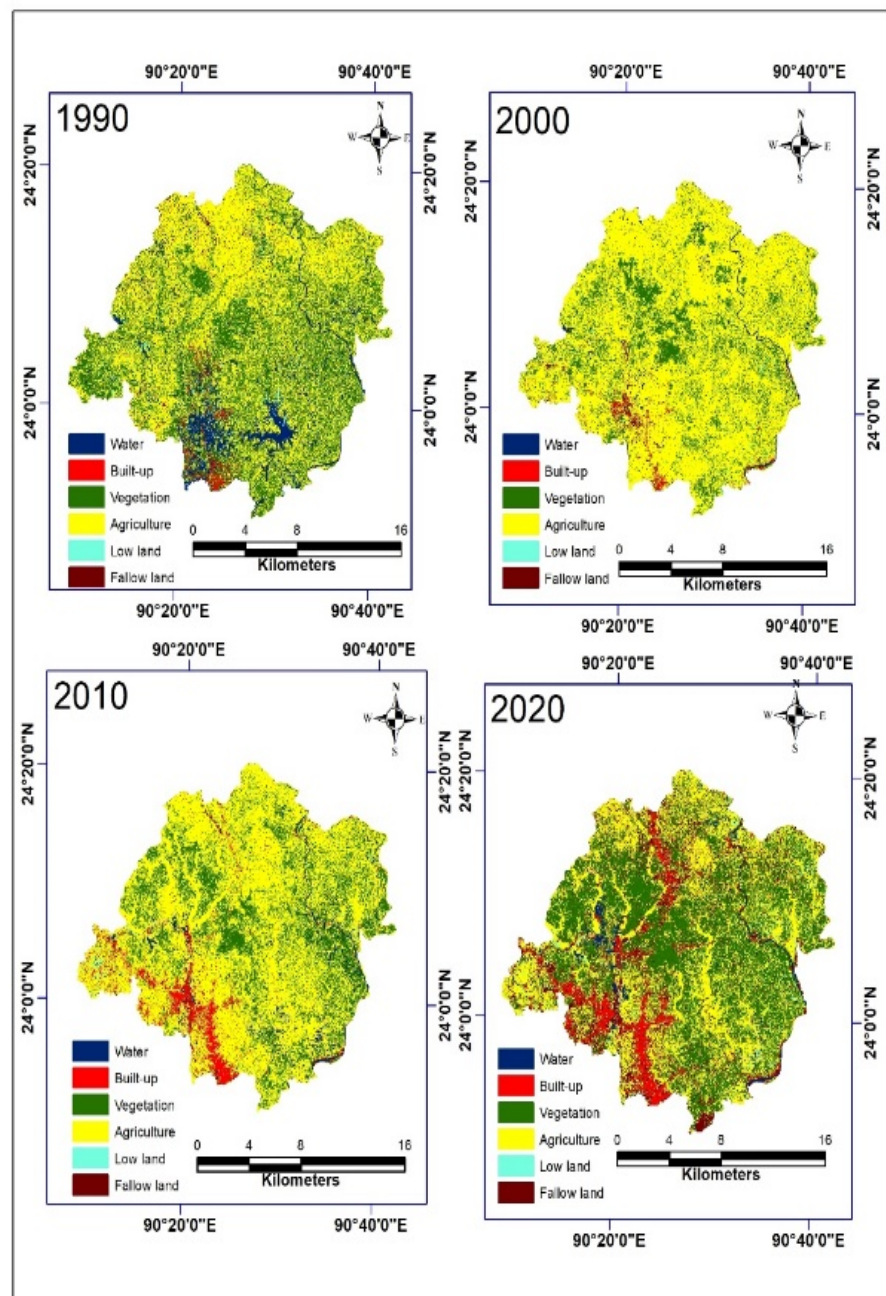


Figure 4. Land-use/land-cover map.

economic activities) connected with population growth in the area. Homestead trees are common in Bangladesh, where they represent a tradition.

4.3. Change Detection

The gain or loss for each individual land class was tabulated to quantify the changes in the area (Figure 6 and Table 6) from 1990 to 2020. During this study period, the built-up area grew by around 87 km². The built-up area acquired area mainly from agricultural (53 km²) and vegetation land (28 km²). Agricultural land lost approximately 264 km², contributing about 398 km² to the vegetation area and 53 km² to the built-up area. Built-up land also gained 230 km² from the vegetation area. The vegetation area gained approximately 105 km² during this period. Overall, the vegetation class acquired about 398 km² from agriculture land and contributed 230 km² to agricultural land.

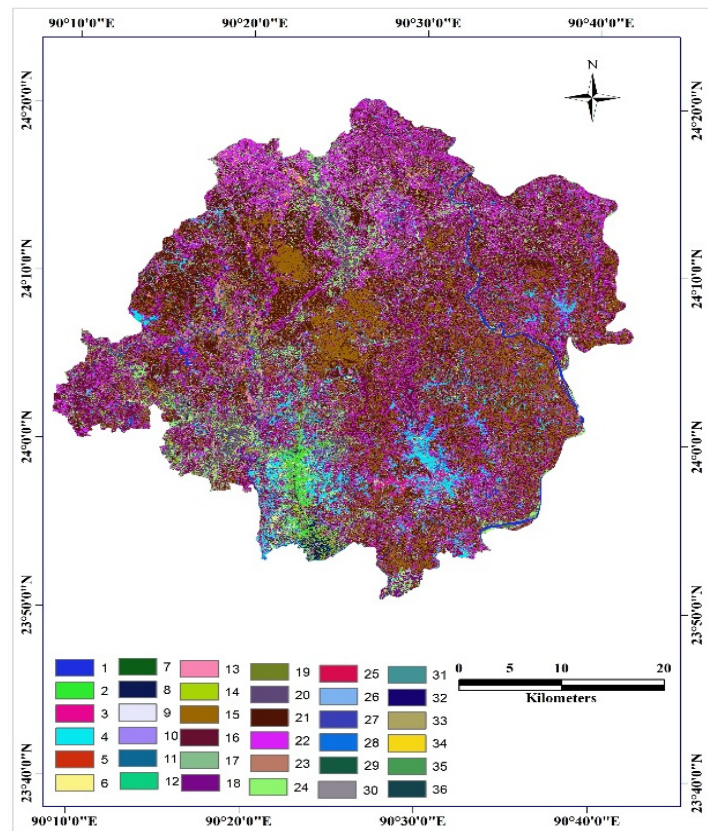


Figure 6. Land-use/land-cover conversion (1990–2020). 1 = W to W, 2 = W to B, 3 = W to V, 4 = W to A, 5 = W to L, 6 = W to F, 7 = B to W, 8 = B to B, 9 = B to V, 10 = B to A, 11 = B to L, 12 = B to F, 13 = V to W, 14 = V to B, 15 = V to V, 16 = V to A, 17 = V to L, 18 = V to F, 19 = A to W, 20 = A to B, 21 = A to V, 22 = A to A, 23 = A to L, 24 = A to F, 25 = L to W, 26 = L to B, 27 = L to V, 28 = L to A, 29 = L to L, 30 = L to F, 31 = F to W, 32 = F to B, 33 = F to V, 34 = F to A, 35 = F to L, 36 = F to F. W = Water, B = Built-up, V = Vegetation, A = Agriculture, L = Low land, F = Fallow land.

Table 6. Changes in land use/land cover (1990–2020).

Change Detection Matrix from 1990 to 2020 (km ²)						
1990–2020	Water	Built-Up	Vegetation	Agriculture	Low Land	Fallow Land
Water	21.69	0.21	12.03	15.98	0.97	0.25
Built-up	12.55	6.52	28.28	52.98	1.73	2.38
Vegetation	26.69	2.62	253.04	398.87	3.20	11.61
Agriculture	85.00	4.72	229.55	368.85	12.01	16.11
Low land	6.48	0.12	10.09	10.38	0.55	0.17
Fallow land	19.03	3.62	58.27	132.90	2.59	7.67

5. Urban Expansion

The Gazipur district is rapidly urbanizing and features the largest city-based corporation in the country. Moreover, Gazipur is the neighboring district to Dhaka, the capital of Bangladesh. Thus, the built-up area of Gazipur continues to increase every year (Figure 7). This district contains the city of Purbachal, the largest housing project of the government of Bangladesh. This project is also playing a significant role in expanding the built-up area of this district.

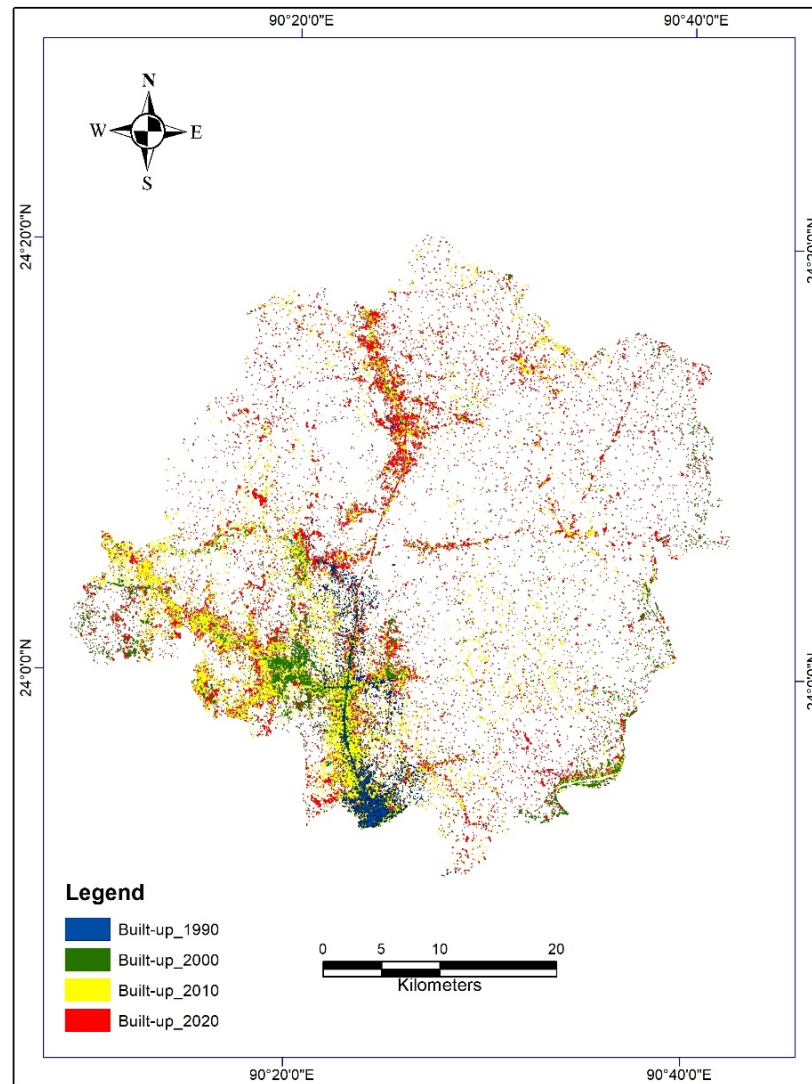


Figure 7. Expansion of built-up area (1990–2020).

5.1. Direction of Urban Expansion

This area features the neighboring city and district of Dhaka, the capital of Bangladesh. Dhaka city is situated in the southern part of the district. Thus, urbanization started from the southern boundary of the city (Figures 8 and 9). The area then expanded toward the south-western and northern directions because the Dhaka bypass is located in the south-western direction and is the regional highway that provides access to the northern part of the country. Another highway runs in the north–south direction. This highway is known as the Dhaka–Mymensingh Highway and connects the greater Mymensingh division (the largest administrative unit) to the capital city of the country. Approximately 40 km² of land is located in the southern fold of the area followed by 22 km² in the south-western fold and 13 km² in the northern fold.

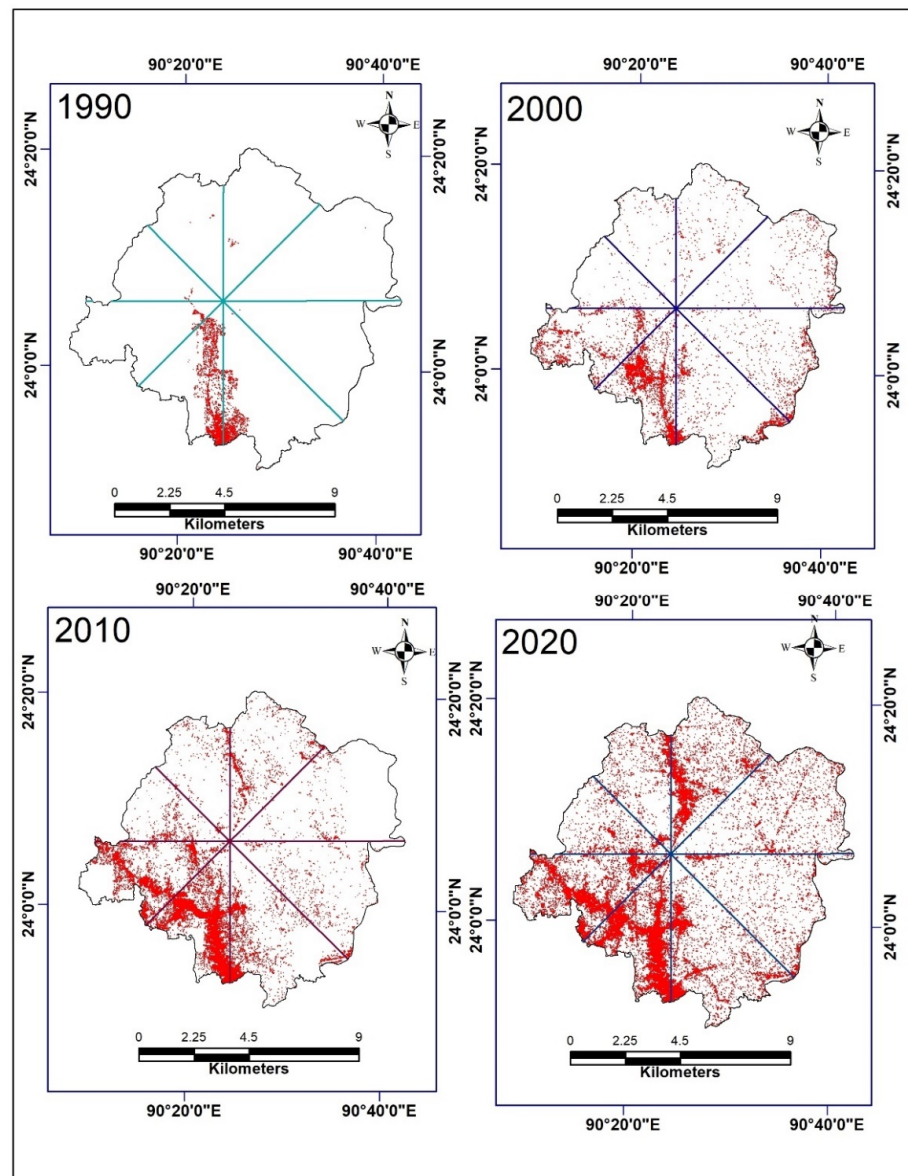


Figure 8. Direction of growth of the built-up area.

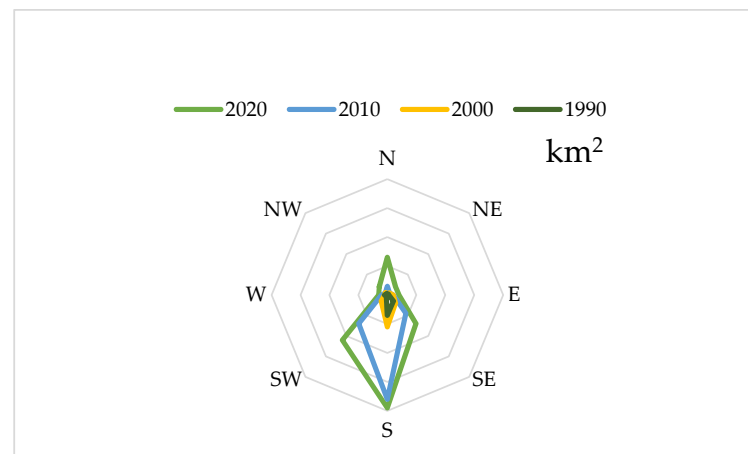


Figure 9. Direction of the built-up land distribution in the study area.

5.2. Distance Assessment of the Urban Expansion

In terms of distance, the area is bound by the five-kilometer-radius circles drawn in Figures 10 and 11. As shown in the built-up map of 2020, the 15-kilometer circle has the largest area among the circles—about 43 km². This zone covers both a part of the Dhaka bypass and a portion of the Dhaka–Mymensingh Highway. The 20-kilometer circle covers 31 km² and is followed by a 25-kilometer circle with a 21-kilometer² area. The central point of the area (i.e., the 5- and 10-kilometer circles) is the lowest area of urbanization (4 and 2 km², respectively), as this part is disconnected from the capital city of the country. This observation indicates that the capital Dhaka has a vital role in developing and expanding the built-up area.

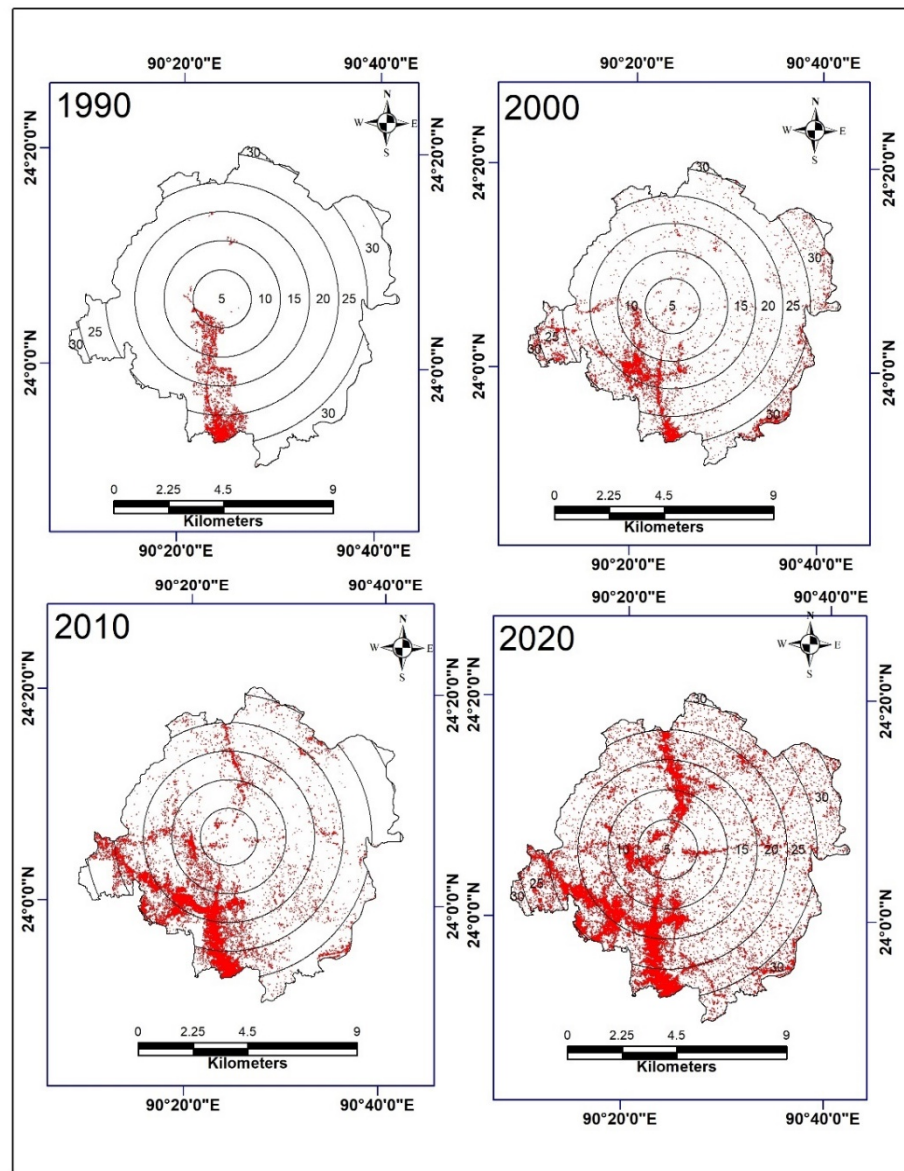


Figure 10. Assessment of built-up area by distance.

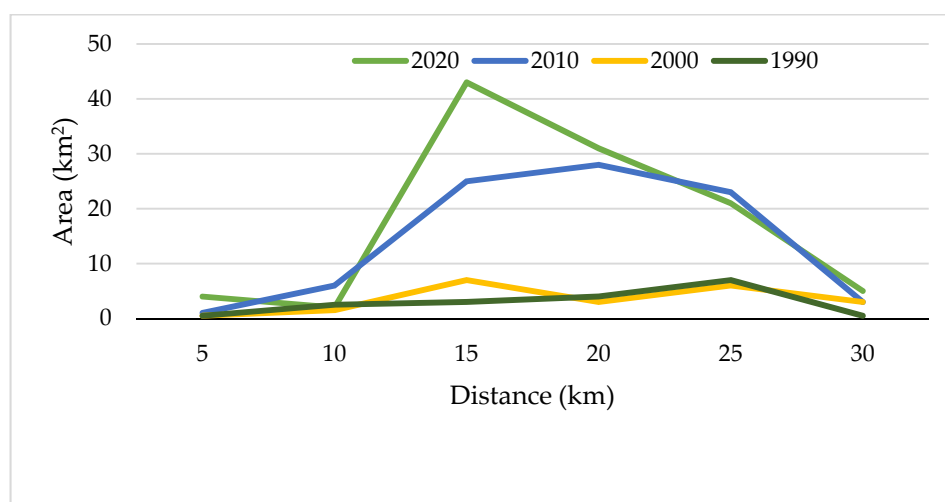


Figure 11. Distribution of built-up area by distance.

6. Driving Factors

6.1. Population Growth

The area is densely populated similarly to the other urban and industrial parts of Bangladesh. According to the Bangladesh Bureau of statistics, the population of the area in 1991, 2001 and 2011 was 1,621,562, 2,031,891 and 3,403,912, respectively [40]. The population density of the area totaled 1231 people/km² in 2001 and increased to 1806 people/km² in 2011. The major built-up area of the district is located in Gazipur Sadar Upazila (subdistrict), which is now under the Gazipur City Corporation area (founded in 2013). In this subdistrict, the population was 588,492, 866,540 and 182,0374 in 1991, 2001 and 2011, respectively [64]. The population rose in this zone by more than three-fold, while the population of the whole district increased by two-fold during the same period. A larger population in the area consumes more land; thus, agricultural land is decreasing while built-up and homestead (part of vegetation) land is increasing.

6.2. Economic Growth

Economic activities are the most significant factors that cause changes in land-use patterns [65]. Bangladesh is now a middle-income country and developing rapidly. Moreover, Bangladesh's per-capita income is increasing with the economic growth of the country. In 2010–2011, the per-capita income of the country was USD 928, while in 2019–2020, that number increased to USD 2064 [66]. Thus, income in Bangladesh grew more than two-fold within nine years. The area under study is an industrial core center [67] featuring thousands of garment factories, a number of pharmaceuticals, an ICT park and other industries. Moreover, there are five universities, four medical colleges and one hospital in the area, and many government organizations, including the Bangladesh Agriculture Research Institute (BARI), Bangladesh Rice Research Institute (BRRI), Security Printing Corporation Limited, Bangladesh Machine Tools Factory and Cantonment are located in the area and contribute to economic activities.

6.3. Location and Accessibility

The area is located the neighborhood district of Dhaka, the capital city of Bangladesh, and is well connected to the city and the rest of the country with a good road network. This factor encourages people to move to this area from different parts of the country. Moreover, the area is located in the Madhupur formation (geological lithology), which is highly suitable for infrastructure development. In terms of geological and geographical aspects, the area is also flood free. Thus, the area's flood-free characteristics, low land price and good communication with the central city are inspiring people to develop the area for both residential and commercial purposes [56]. A part of Purbachal, one of the largest

housing ventures operated by the government, is located in Gazipur district due to its suitable location and well-connected road network. Additionally, many recreational parks and film/drama shooting locations can be found in the area.

7. Conclusions

This study aimed to quantify land-use/land-cover changes and urban spread by using remote sensing and GIS technologies along with multi-temporal Landsat imagery of the Gazipur district, Bangladesh, during 1990 to 2020. This study also uncovered the impact of economic and population growth on changes in the conventional land-use/land-cover arrangement of the area. The overall outcomes of the study indicate that agricultural land experienced maximum modifications over this time period, with a total reduction in agricultural land of 264 km². The vegetation and built-up area showed increasing trends, but vegetation land increased due to the homestead planting of trees, which is a regular phenomenon in Bangladesh. This result also suggests that the increasing trend of population is one of the key factors underlying land-use changes. The built-up area grew by approximately five-fold (18 to 104 km²) during the study period, indicating significant urbanization. Economic growth, location and accessibility were observed to be the most important elements that enhanced the urban area, while agricultural land contributed the most to urban growth. The urban area was largest during 2000 to 2010. In 2020, fallow land became larger (224 km²), but this was a transitional effect of urbanization. Purbachal, the largest government housing project, was also shown to be fallow in this analysis, due to its provisional change phase. Urban expansion demonstrated spreading through both the active built-up area and the main transport routes, including the Dhaka bypass and the Dhaka–Mymensingh Highway, as commonly found around large Asian cities, including the Chinese capital of Beijing and the Japanese capital of Tokyo [68,69]. The results of this study provide a complete description of the area for the stakeholders and policymakers who will realize the Bangladesh government’s plan to transform rural areas into urban areas, thereby facilitating appropriate considerations of environmental issues in respect of sustainable development goal 11.

Author Contributions: Conceptualization, H.M.A.; methodology, H.M.A.; software, K.P.; validation, K.P.; formal analysis, H.M.A.; investigation, K.T. and A.M.; resources, A.M.; data curation, N.Y.; writing—original draft preparation, H.M.A.; writing—review and editing, N.Y. and C.Y.; visualization, K.P. and W.J.; supervision, K.T. and A.M.; project administration, K.T.; funding acquisition, W.J. All authors have read and agreed to the published version of the manuscript.

Funding: This research was partially supported by “Thailand Science Research and Innovation” (TSRI). Grant Number: ENV6405051S.

Data Availability Statement: Not applicable.

Acknowledgments: The authors would like to thankfully acknowledge research Grants from Thailand’s Interdisciplinary Graduate School of Energy System (Contract No. IGS-Energy 1/2019/02) funds for Ph.D. research in Sustainable Energy Management, Faculty of Environmental Management, Graduate School, Prince of Songkla University, Thailand. The authors also express their gratitude to Mohammad Lutful Kabir for his assistance during field research in Bangladesh.

Conflicts of Interest: The authors declare no conflict of interest.

References

1. European Environmental Agency (EEA). *Urban Sprawl in Europe Joint EEA-FOEN Report*; European Environmental Agency—Swiss Federal Office for the Environment: Ittigen, Switzerland, 2016. Available online: <https://www.eea.europa.eu/publications/urban-sprawl-in-europe> (accessed on 20 March 2021).
2. Goswami, M. Conceptualizing Peri-Urban-Rural Landscape Change for Sustainable Management. Available online: <http://www.isec.ac.in/WP%20425%20-%20Mrinalini%20Goswami%20-%20Final.pdf> (accessed on 10 January 2020).
3. Alipbeki, O.; Alipbekova, C.; Sterenharz, A.; Toleubekova, Z.; Aliyev, M.; Mineyev, N.; Amangaliyev, K. A Spatiotemporal Assessment of Land Use and Land Cover Changes in Peri-Urban Areas: A Case Study of Arshaly District, Kazakhstan. *Sustainability* **2020**, *12*, 1556. [CrossRef]

4. World Bank. Urban Population Growth. 2019. Available online: <https://data.worldbank.org/indicator/SP.URB.GROW> (accessed on 10 October 2021).
5. Mansour, S.; Al-Belushi, M.; Al-Awadhi, T. Monitoring land use and land cover changes in the mountainous cities of Oman using GIS and CA-Markov modelling techniques. *Land Use Policy* **2020**, *91*, 104414. [[CrossRef](#)]
6. Acheampong, M.; Yu, Q.; Enomah, L.D.; Anchang, J.; Eduful, M. Land use/cover change in Ghana's oil city: Assessing the impact of neoliberal economic policies and implications for sustainable development goal number one—A remote sensing and GIS approach. *Land Use Policy* **2018**, *73*, 373–384. [[CrossRef](#)]
7. Matlhodi, B.; Kenabatho, P.K.; Parida, B.P.; Maphanyane, J.G. Evaluating Land Use and Land Cover Change in the Gaborone Dam Catchment, Botswana, from 1984–2015 Using GIS and Remote Sensing. *Sustainability* **2019**, *11*, 5174. [[CrossRef](#)]
8. Yekeen, S.T.; Balogun, A.-L. Advances in Remote Sensing Technology, Machine Learning and Deep Learning for Marine Oil Spill Detection, Prediction and Vulnerability Assessment. *Remote Sens.* **2020**, *12*, 3416. [[CrossRef](#)]
9. Afrin, S.; Gupta, A.; Farjad, B.; Ahmed, M.R.; Achari, G.; Hassan, Q.K. Development of Land-Use/Land-Cover Maps Using Landsat-8 and MODIS Data, and Their Integration for Hydro-Ecological Applications. *Sensors* **2019**, *19*, 4891. [[CrossRef](#)]
10. Phiri, D.; Morgenroth, J. Developments in Landsat Land Cover Classification Methods: A Review. *Remote Sens.* **2017**, *9*, 967. [[CrossRef](#)]
11. Khatancharoen, C.; Tsuyuki, S.; Bryanin, S.; Sugiura, K.; Seino, T.; Lisovsky, V.; Borisova, I.; Wada, N. Long-Time Interval Satellite Image Analysis on Forest-Cover Changes and Disturbances around Protected Area, Zeya State Nature Reserve, in the Russian Far East. *Remote Sens.* **2021**, *13*, 1285. [[CrossRef](#)]
12. Das, S.; Angadi, D.P. Land use land cover change detection and monitoring of urban growth using remote sensing and GIS techniques: A micro-level study. *Geo J.* **2021**, *2021*, 1–23. [[CrossRef](#)]
13. Sefrin, O.; Riese, F.; Keller, S. Deep Learning for Land Cover Change Detection. *Remote Sens.* **2020**, *13*, 78. [[CrossRef](#)]
14. Vinayak, B.; Lee, H.; Gede, S. Prediction of Land Use and Land Cover Changes in Mumbai City, India, Using Remote Sensing Data and a Multilayer Perceptron Neural Network-Based Markov Chain Model. *Sustainability* **2021**, *13*, 471. [[CrossRef](#)]
15. Rawat, J.; Kumar, M. Monitoring land use/cover change using remote sensing and GIS techniques: A case study of Hawalbagh block, district Almora, Uttarakhand, India. *Egypt. J. Remote Sens. Space Sci.* **2015**, *18*, 77–84. [[CrossRef](#)]
16. Hathout, S. The use of GIS for monitoring and predicting urban growth in east and west St Paul, Winnipeg, Manitoba, Canada. *J. Environ. Manag.* **2002**, *66*, 229–238. [[CrossRef](#)]
17. Herold, M.; Goldstein, N.C.; Clarke, K. The spatiotemporal form of urban growth: Measurement, analysis and modeling. *Remote Sens. Environ.* **2003**, *86*, 286–302. [[CrossRef](#)]
18. Lambin, E.F.; Geist, H.J.; Lepers, E. Dynamics of land-use and land-cover change in tropical regions. *Annu. Rev. Environ. Resour.* **2003**, *28*, 205–241. [[CrossRef](#)]
19. Shi, G.; Jiang, N.; Yao, L. Land Use and Cover Change during the Rapid Economic Growth Period from 1990 to 2010: A Case Study of Shanghai. *Sustainability* **2018**, *10*, 426. [[CrossRef](#)]
20. Fonji, S.F.; Taff, G.N. Using satellite data to monitor land-use land-cover change in North-eastern Latvia. *SpringerPlus* **2014**, *3*, 61. [[CrossRef](#)]
21. Tran, H.; Tran, T.; Kervyn, M. Dynamics of land cover/land use changes in the Mekong Delta, 1973–2011: A remote sensing analysis of the Tran Van Thoi District, Ca Mau Province, Vietnam. *Remote Sens.* **2015**, *7*, 2899–2925. [[CrossRef](#)]
22. Akinyemi, F.O. Land change in the central Albertine rift: Insights from analysis and mapping of land use-land cover change in north-western Rwanda. *Appl. Geogr.* **2017**, *87*, 127–138. [[CrossRef](#)]
23. Kale, M.P.; Chavan, M.; Pardeshi, S.; Joshi, C.; Verma, P.A.; Roy, P.S.; Srivastav, S.K.; Jha, A.K.; Chaudhari, S.; Giri, Y.; et al. Land-use and land-cover change in Western Ghats of India. *Environ. Monit. Assess.* **2016**, *188*, 1–23. [[CrossRef](#)]
24. Arowolo, A.O.; Deng, X. Land use/land cover change and statistical modelling of cultivated land change drivers in Nigeria. *Reg. Environ. Chang.* **2018**, *18*, 247–259. [[CrossRef](#)]
25. Hussain, S.; Mubeen, M.; Akram, W.; Ahmad, A.; Habib-Ur-Rahman, M.; Ghaffar, A.; Amin, A.; Awais, M.; Farid, H.U.; Farooq, A.; et al. Study of land cover/land use changes using RS and GIS: A case study of Multan district, Pakistan. *Environ. Monit. Assess.* **2019**, *192*, 2. [[CrossRef](#)] [[PubMed](#)]
26. Alijani, Z.; Hosseinali, F.; Biswas, A. Spatio-temporal evolution of agricultural land use change drivers: A case study from Chalous region, Iran. *J. Environ. Manag.* **2020**, *262*, 110326. [[CrossRef](#)]
27. Dewan, A.; Yamaguchi, Y. Land use and land cover change in Greater Dhaka, Bangladesh: Using remote sensing to promote sustainable urbanization. *Appl. Geogr.* **2009**, *29*, 390–401. [[CrossRef](#)]
28. Jat, M.K.; Garg, P.K.; Khare, D. Monitoring and modelling of urban sprawl using remote sensing and GIS techniques. *Int. J. Appl. Earth Obs. Geoinf.* **2008**, *10*, 26–43. [[CrossRef](#)]
29. Mundia, C.N.; Aniya, M. Dynamics of landuse/cover changes and degradation of Nairobi City, Kenya. *Land Degrad. Dev.* **2006**, *17*, 97–108. [[CrossRef](#)]
30. Liu, X.; Lathrop, R., Jr. Urban change detection based on an artificial neural network. *Int. J. Remote Sens.* **2002**, *23*, 2513–2518. [[CrossRef](#)]
31. Habitat, U. *The State of the World's Cities 2001*; United Nations for Human Settlements: Nairobi, Kenya, 2001.
32. Ishtiaque, A.; Shrestha, M.; Chhetri, N. Rapid Urban Growth in the Kathmandu Valley, Nepal: Monitoring Land Use Land Cover Dynamics of a Himalayan City with Landsat Imageries. *Environments* **2017**, *4*, 72. [[CrossRef](#)]

33. Goldblatt, R.; Stuhlmacher, M.F.; Tellman, B.; Clinton, N.; Hanson, G.; Georgescu, M.; Wang, C.; Serrano-Candela, F.; Khandelwal, A.K.; Cheng, W.-H.; et al. Using Landsat and nighttime lights for supervised pixel-based image classification of urban land cover. *Remote Sens. Environ.* **2018**, *205*, 253–275. [CrossRef]
34. Thapa, R.B.; Murayama, Y. Examining Spatiotemporal Urbanization Patterns in Kathmandu Valley, Nepal: Remote Sensing and Spatial Metrics Approaches. *Remote Sens.* **2009**, *1*, 534–556. [CrossRef]
35. Ahmad, F.; Goparaju, L.; Qayum, A. LULC analysis of urban spaces using Markov chain predictive model at Ranchi in India. *Spat. Inf. Res.* **2017**, *25*, 351–359. [CrossRef]
36. Dewan, A.M.; Yamaguchi, Y. Using remote sensing and GIS to detect and monitor land use and land cover change in Dhaka Metropolitan of Bangladesh during 1960–2005. *Environ. Monit. Assess.* **2008**, *150*, 237–249. [CrossRef]
37. Haque, M.I.; Basak, R. (Eds.) *Land Cover Change Detection Using GIS and Remote Sensing Techniques: A Spatio-Temporal Study on Tanguar Haor, Sunamganj, Bangladesh*. 2016 International Conference on Innovations in Science, Engineering and Technology (ICISSET); IEEE: Piscataway Township, NJ, USA, 2016.
38. Chowdhury, M.; Hasan, M.E.; Al Mamun, M.M.A. Land use/land cover change assessment of Halda watershed using remote sensing and GIS. *Egypt. J. Remote Sens. Space Sci.* **2020**, *23*, 63–75. [CrossRef]
39. World Bank. 2020. Available online: [Data.worldbank.org/indicator/NY.GDP.MKTP.KD.ZG?locations=BD](https://data.worldbank.org/indicator/NY.GDP.MKTP.KD.ZG?locations=BD) (accessed on 16 November 2020).
40. *District Statistics 2011, Gazipur*; Bangladesh Bureau of Statistics: Dhaka, Bangladesh, 2011.
41. Paul, S.S. Analysis of Land Use and Land Cover Change in Kiskatinaw River Watershed: A Remote Sensing, Gis & Modeling Approach. Masters' Thesis, University of Northern British Columbia, Prince George, BC, Canada, 2013.
42. Paiboonvorachat, C. Using Remote Sensing and GIS Techniques to Assess Land Use/Land Cover Changes in the Nan Watershed, Thailand. Masters' Thesis, Southern Illinois University at Carbondale, Carbondale, IL, USA, 2008.
43. Campbell, B.J. *Introduction to Remote Sensing*, 3rd ed.; Guilford Press: New York, NY, USA, 2002.
44. Chen, D.; Stow, D. The effect of training strategies on supervised classification at different spatial resolutions. *Photogramm. Eng. Remote Sens.* **2002**, *68*, 1155–1162.
45. Jensen, J.R. *Introductory Digital Image Processing: A Remote Sensing Perspective*; Prentice-Hall Inc.: Hoboken, NJ, USA, 1996.
46. Congalton, R.G. A review of assessing the accuracy of classifications of remotely sensed data. *Remote Sens. Environ.* **1991**, *37*, 35–46. [CrossRef]
47. Harris, P.M.; Ventura, S.J. The integration of geographic data with remotely sensed imagery to improve classification in an urban area. *Photogramm. Eng. Remote Sens.* **1995**, *61*, 993–998.
48. Hassan, M.M.; Nazem, M.N.I. Examination of land use/land cover changes, urban growth dynamics, and environmental sustainability in Chittagong city, Bangladesh. *Environ. Dev. Sustain.* **2016**, *18*, 697–716. [CrossRef]
49. Hassan, M.M. Monitoring land use/land cover change, urban growth dynamics and landscape pattern analysis in five fastest urbanized cities in Bangladesh. *Remote Sens. Appl. Soc. Environ.* **2017**, *7*, 69–83. [CrossRef]
50. Yuan, F.; Sawaya, K.E.; Loeffelholz, B.C.; Bauer, M.E. Land cover classification and change analysis of the Twin Cities (Minnesota) Metropolitan Area by multitemporal Landsat remote sensing. *Remote Sens. Environ.* **2005**, *98*, 317–328. [CrossRef]
51. Rutherford, G.N.; Bebi, P.; Edwards, P.J.; Zimmermann, N. Assessing land-use statistics to model land cover change in a mountainous landscape in the European Alps. *Ecol. Model.* **2008**, *212*, 460–471. [CrossRef]
52. Weng, Q. Remote sensing of impervious surfaces in the urban areas: Requirements, methods, and trends. *Remote Sens. Environ.* **2012**, *117*, 34–49. [CrossRef]
53. Deilmai, B.R.; Bin Ahmad, B.; Zabihi, H. Comparison of two Classification methods (MLC and SVM) to extract land use and land cover in Johor Malaysia. *IOP Conf. Ser. Earth Environ. Sci.* **2014**, *20*, 1–6. [CrossRef]
54. Xu, X.; Min, X. Quantifying spatiotemporal patterns of urban expansion in China using remote sensing data. *Cities* **2013**, *35*, 104–113. [CrossRef]
55. Qian, Y.; Zhou, W.; Yan, J.; Li, W.; Han, L.; Kerle, N.; Gerke, M.; Lefevre, S. Comparing machine learning classifiers for object-based land cover classification using very high resolution imagery. *GEOBIA 2016 Solut. Synerg.* **2016**, *7*, 153–168. [CrossRef]
56. Hasan, M.M.; Southworth, J. Analyzing land cover change and urban growth trajectories of the mega-urban region of Dhaka using remotely sensed data and an ensemble classifier. *Sustainability* **2018**, *10*, 10. [CrossRef]
57. Hong, Z.; Hailin, L.; Zhen, C. Analysis of Land Use Dynamic Change and Its Impact on the Water Environment in Yunnan Plateau Lake Area — A Case Study of the Dianchi Lake Drainage Area. *Procedia Environ. Sci.* **2011**, *10*, 2709–2717. [CrossRef]
58. Senseman, G.M.; Bagley, C.F.; Tweddale, S.A. *Accuracy Assessment of the Discrete Classification of Remotely-Sensed Digital Data for Landcover Mapping*; Construction Engineering Research Lab (Army) Champaign IL: Springfield, VA, USA, 1995.
59. Mishra, P.K.; Rai, A.; Rai, S.C. Land use and land cover change detection using geospatial techniques in the Sikkim Himalaya, India. *Egypt. J. Remote Sens. Space Sci.* **2020**, *23*, 133–143. [CrossRef]
60. Pawe, C.K.; Saikia, A. Unplanned urban growth: Land use/land cover change in the Guwahati Metropolitan Area, India. *Geogr. Tidsskr. J. Geogr.* **2018**, *118*, 88–100. [CrossRef]
61. Sun, C.; Wu, Z.; Lv, Z.; Yao, N.; Wei, J. Quantifying different types of urban growth and the change dynamic in Guangzhou using multi-temporal remote sensing data. *Int. J. Appl. Earth Obs. Geoinf.* **2013**, *21*, 409–417. [CrossRef]
62. Pandey, B.; Seto, K.C. Urbanization and agricultural land loss in India: Comparing satellite estimates with census data. *J. Environ. Manag.* **2015**, *148*, 53–66. [CrossRef] [PubMed]

63. Hegazy, I.R.; Kaloop, M.R. Monitoring urban growth and land use change detection with GIS and remote sensing techniques in Daqahlia governorate Egypt. *Int. J. Sustain. Built Environ.* **2015**, *4*, 117–124. [[CrossRef](#)]
64. Population.de C. Gazipur Population. Available online: https://citypopulation.de/en/bangladesh/dhaka/3330__gazipur_sadar/ (accessed on 12 November 2020).
65. Xu, X.; Jain, A.K.; Calvin, K.V. Quantifying the biophysical and socioeconomic drivers of changes in forest and agricultural land in South and Southeast Asia. *Glob. Chang. Biol.* **2019**, *25*, 2137–2151. [[CrossRef](#)] [[PubMed](#)]
66. Sukhbor, S.A. Daily Prothom Alo (National Bangla Newspaper of Bangladesh). *Good News in Crisis Time*, 6 November.
67. Rahman, S.; Mohiuddin, H.; Al Kafy, A.; Sheel, P.K.; Di, L. Classification of cities in Bangladesh based on remote sensing derived spatial characteristics. *J. Urban Manag.* **2019**, *8*, 206–224. [[CrossRef](#)]
68. Liu, S.; Wu, C.; Shen, H. A GIS based model of urban land use growth in Beijing. *Acta Geogr. Sin.-Chin. Ed.* **2000**, *55*, 416–426.
69. Sorensen, A. Land readjustment and metropolitan growth: An examination of suburban land development and urban sprawl in the Tokyo metropolitan area. *Prog. Plan.* **2000**, *53*, 217–330. [[CrossRef](#)]